2023 IEEE/ASME International Conference on Advanced Intelligent Mechatronics (AIM)
June 28-30, 2023. Seattle, Washington, USA

Semi-active magnetorheological suspension of a full-vehicle model based on combined vertical and attitude control

1st Peng Lyv
Engineering College
Ocean University of China
Qingdao, China
ouclp@stu.ouc.edu.cn

2nd Dingxin Leng*
Engineering College
Ocean University of China
Qingdao, China
lengdingxin@126.com

3rd Yancheng Li
School of Civil and Environmental Engineering, University of Technology Sydney, NSW, Australia
Yancheng.Li@uts.edu.au

4th Tiancheng Xu
Shenzhen Chao-Shang Technology Corporation,
Shenzhen, China
xutiancheng@upwardtech.cn

5th Wang Huixing
Department of Mechanical Engineering
Nanjing, China
huixing_wang@163.com

6th Hanou Xu
Shenzhen Chao-Shang Technology Corporation,
Shenzhen,
xuhanou@upwardtech.cn

***Abstract*—The present work proposes a novel control algorithm of semi-active magnetorheological (MR) suspension for full vehicle vibration suppression. The mathematical model of full vehicle with seven-degrees-of-freedom is established and its vibration mode analysis is conducted. The proposed controller derives the desired current for individual MR damper by mitigating the vertical motion of vehicle body and the body attitude adjustment. Compared with existing control algorithms, the proposed controller can avoid complex inverse model of MR damper and force tracing issue. The semi-active control effectiveness is evaluated. The results show that the vehicle body acceleration, pitch and roll angle are greatly reduced by the proposed controller.**

Keywords—Combined vertical and attitude control, magnetorheological suspension, ride comfort, full-vehicle control

I. INTRODUCTION

Suspension system of a vehicle is significant for maintaining the ride comfort and steering stability, which isolates the unwanted vibration from the roads. In the past, the passive damper based suspension has been widely investigated and applied. However, its performance may only be effective in a narrow frequency range due to its fixed parameters (e.g., spring and damping coefficients); and one has to find trade-off between the ride comfort and vehicle handling. Therefore, a low-cost adaptive damper is being actively developed, which could provide the variable damping force with the variation of road conditions and the requirement of vehicle state. Semi-active damper is a typical adaptive damper with advantages of active and passive suspensions, which can change the damping parameters and present the fail-safe characteristics with low energy consumption. Recently, semi-active magnetorheological fluids (MRF) damper whose viscosity can be varied by applying different current has been paid increasingly attention.

For suspension system with MR dampers, developing a control algorithm to fully utilize the great potential of the MR damper is of ultimate significance for practical application. In the last decade, various control methods have been proposed[1-9]. The present studies are mainly focused on the quarter-car vertical suppression, which deals with the conflicts between the reduction of sprung mass acceleration and ride stability. However, in reality, besides the vertical vibration, the full vehicle also presents pitch and roll motions, that is, the attitude state variation. Merely control for each suspension of quarter-car model (e.g., normally two-degree-of-freedom) cannot eliminate the angular motion from different degrees of freedom (DOF) of full vehicle attitude, which even deteriorates the vehicle body vertical vibration. Therefore, the combined vertical and attitude control for the full vehicle dynamics should be investigated for the practical application.

For full vehicle-suspension dynamics control, some studies are conducted on the decoupling and layered controller design. Yao et al proposed a decoupling skyhook controller for MRF suspension, in which vehicle body motion in terms of vertical, pitch and roll have been controlled by three skyhook controller and the corresponding control force were converted into a combined damping force for each damper[10]. Wang et al designed an attitude compensation controller for full vehicle body, in which the sky-hook control force and the attitude compensation force of each suspension was calculated for

Corresponding author:
Department of mechanical and electrical engineering, Ocean University of China, Qingdao, 266100, China. Tel.: +86-0532-66781131; fax: +86-0532-66781131.
E-mail address: lengdingxin@ouc.edu.cn (D.X. Leng).
This research was financially funded by Shenzhen Upward Tech Co. Ltd.

suppressing the sprung mass vibration[11].Additionally, some researchers proposed cooperative controllers among the suspension system, steering system and braking system[12-14]. However, the above mentioned control methods are hardly implemented due to the complexity, that is, the output of these controllers is the damping force for individual MRF damper, which needs an accurate inverse model to derive the desired current for each damper. Inverse models are normally established by non-physical method (e.g., neutral-based model); the error of the inverse model impedes the accurate tracing of damping force, and the bumping effect between minimum and maximum currents may present due to the non-physical model's discontinuity. Consequently, it is significant to develop a practicable control algorithm which directly outputs the desired current for MRF damper instead of the controllable damping force in the full vehicle dynamics design.

In the present work, a feasible implemented controller has been developed for controlling the attitude and vertical vibration of the full vehicle. The proposed control algorithm is based on the modified skyhook control of each MRF damper and the vehicle attitude is also compensated based on the real-time motion of individual damper. The most highlight is that this proposed controller can directly derive the desired current for MRF damper for its practical implementation. The remainder of this paper is organized as follows. Firstly, a full vehicle model with nonlinear MRF damper model is established. The random road disturbance is considered as input. Secondly, the dynamic characteristics of a manufactured MRF damper are described and its accurate model is developed. Thirdly, a novel controller is presented by fully considering the vertical mitigation and attitude compensation of the practical vehicle. Finally, evaluation of control performance is presented and the main conclusions are summarized.

II. FULL VEHICLE MODEL

A. 7-DOF vehicle-suspension model

A seven-degree-of-freedom full vehicle model of the semi-active suspension system is established, which consists of the body and four wheels (Fig. 1). The vertical, roll and pitch motions of the vehicle body constitute three degrees of freedom, and the vertical motions of each wheel constitute another four degrees of freedom.

The dynamic equation of the full vehicle model is expressed as follows,

$$M\ddot{z}_g = \sum_{i=1}^{4} F_{si} - \sum_{i=1}^{4} F_{MRi} \tag{1}$$

$$I_y\ddot{\theta} = l_f\left(F_{s1} - F_{MR1} + F_{s2} - F_{MR2}\right) - l_r\left(F_{s3} - F_{MR3} + F_{s4} - F_{MR4}\right) \tag{2}$$

$$I_x\ddot{\phi} = \frac{b_f}{2}\left[\left(F_{s1} - F_{MR1}\right) - \left(F_{s2} - F_{MR2}\right)\right] + \frac{b_r}{2}\left[\left(F_{s3} - F_{MR3}\right) - \left(F_{s4} - F_{MR4}\right)\right] \tag{3}$$

$$m_i\ddot{z}_{usi} = -k_{ti}\left(z_{usi} - z_i\right) - F_{si} + F_{MRi} \tag{4}$$

where,

$$F_{si} = -k_{si}\left(z_{si} - z_{usi}\right) - c_{si}\left(\dot{z}_{si} - \dot{z}_{usi}\right) \tag{5}$$

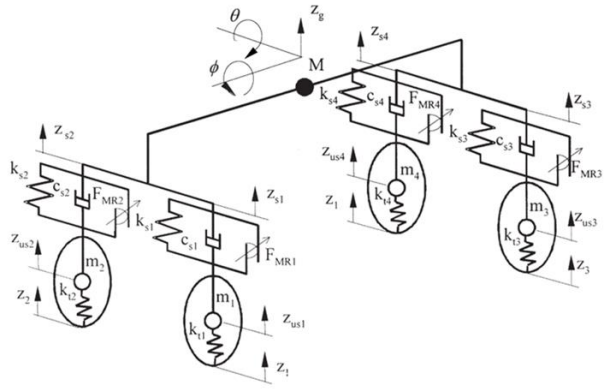

Fig. 1. Full vehicle model of MR suspension system

Displacement of the sprung mass at each suspension position (z_{s1}, z_{s2}, z_{s3}, z_{s4}) can be derived by z_g, l_f, l_r, b_f, b_r, θ and ϕ [11]. In the above equation, M is the sprung mass and $m_i\ (i=1,2,3,4)$ is the unsprung mass. In the present work, $i=1,2,3,4$ corresponds to left front, right front, left rear and right rear suspension. I_y and I_x are the rotational inertia of the vehicle around the pitch axis and the roll axis respectively. k_{si} is the spring stiffness coefficient of the suspension. c_{si} is the equivalent damping coefficient produced by the suspension structure; k_{ti} is the equivalent stiffness coefficient of the tire. z_g, z_{usi} and z_i are the vertical displacement of the vehicle body, the unsprung mass and the road excitation signal, respectively. θ and ϕ are the pitch angle and roll angle of the vehicle respectively. l_f and l_r are the distances between the front and rear axles and the vehicle centroid, and b_f and b_r are the wheelbases of the front and rear axles, respectively.

B. Random road profile

Random road excitation is considered in the present work. In practical, the road profile is a typical irregular signal. As the standard of ISO 8608, the random road profile is derived in the term of power spectrum density (PSD) by Wiener-Khinchin theory[12]. In the present work, the road roughness is chosen by Class D. The vehicle velocity v is 40 km/h. It is assumed that the phase delay of the random road profile can be expressed in Gaussian density. The road excitation of one single wheel is[15]:

$$\dot{q}(t) = -2\pi n_1 \cdot q(t) + 2\pi\sqrt{G_0\mu}\cdot\omega(t) \tag{10}$$

where, n_1 is the lower cut-off frequency, 0.01Hz; G_0 is the road roughness coefficient; $\omega(t)$ is unit Gaussian white noise.

By considering the coherence of the left and right wheels, two different random road profiles are designed for the left and right sides of the vehicle. The front and rear profiles are derived by regarding the phase delay related to the vehicle length and driving velocity.

C. Key parameters for full vehicle–suspension system

In the present work, the key parameters of a full vehicle model with suspension are taken from a middle weight class vehicle. The body mass (M) of this model is 2042.3 kg, with a front unsprung mass (m_1, m_2) of 173.2 kg and a rear unsprung

mass (m_3, m_4) of 193.9 kg. The distance from the vehicle center of mass to the vehicle (l_f) is 1.2496 m, and the distance to the rear of the vehicle (l_r) is 1.4984 m. The front wheelbase (b_f) and rear wheelbase (b_r) are 1.615 m and 1.61 m respectively. Its rolling moment of inertia (I_x) and pitching moment of inertia (I_y) are 955 kg· m² and 3761.5 kg ·m², respectively. The equivalent stiffness of the coil springs for the front (k_{s1}, k_{s2}) and rear suspensions is 35940 N/m and 26685 N/m, respectively. Considering the tire as a constant stiffness spring, the equivalent stiffness of the four tires (k_{t1}, k_{t2}, k_{t3}, k_{t4}) is 278000 N/m.

The original damping coefficient of a passive damper (1800 Ns/m) is utilized in the simulation for comparison with the MRF suspension system. Referred by the Choi's work[16], the optimal damping coefficient for the adopted full-vehicle model is determined by the transmissibility index which is the ratio between amplitude of the road excitation and sprung mass. In the present work, the optimal damping variation range is adopted as 1200 or 2700 Ns/m.

D. Vibration mode analysis of full-vehicle model

The vibration mode of a full-vehicle system is essential for identifying its resonance source. The vibration frequency and mode shape can be derived by the eigenvalues and eigenvectors of the dynamic model. It can be seen that the sprung mass resonance focus on the low frequency (e.g., in the range of 1-2 Hz), that is, the heave, pitch and roll resonance frequency values of the sprung mass are 1.15 Hz, 1.21 Hz and 1.39 Hz respectively. While for the unsprung mass, the resonance is in the high frequency range (e.g., 5 Hz ~ 7 Hz) and the main vibration mode shapes are twist and bending, that is, the resonance frequency values are 6.31 Hz, 6.32 Hz, 6.78 Hz and 6.79 Hz. It is noted that by adding the damping of four MRF dampers, the exact resonance frequency of the full vehicle should be slightly changed, while the fundamental vibration mode is still identical. The desired semi-active damper should present the variable damping effect to mitigate the sprung and unsprung mass vibration.

III. MR DAMPER MODEL

Based on the optimal damping value, an MRF damper is designed and manufactured, as shown in Fig. 2. The damper has a twin-tube structure, which consists of chamber with piston and MR fluids. When the piston moves in the axial direction, MR fluids moves in the chamber. Along the MRF flow direction, a magnetic field is applied and the field strength is controlled by the current signal. As the damping value of MRF changed, the damping force is adjusted.

Fig. 2. Configuration of the proposed MRF damper

In the present work, the damping force of MRF damper is depicted by a hyperbolic tangent model[17],

$$F = \alpha \tanh\left(\beta \dot{x} + \delta sign\left(x\right)\right) + c\dot{x} + kx + f_0 \qquad (11)$$

where α is the proportionality coefficient of hysteresis curve; β is the proportional coefficient of the slope of hysteresis curve; δ is the half width of hysteresis curve; c is damping coefficient; k is the stiffness coefficient; f_0 is the bias force; x is the displacement.

The dynamic characteristic of MRF damper is experimentally tested. The non-contact displacement sensor and force sensor are assembled in the testing system, which records the force-displacement data. Different current signals are applied from 0.0 A to 1.0 A with increment of 3.0 A. The velocities are calculated by the difference approximation method of displacement and sampling frequency. Based on the tested data, the key parameters of the hyperbolic tangent model are identified. Under the amplitude of 4 mm harmonic excitation with 4 Hz, the experimental force-displacement and force-velocity hysteresis loops are shown in Fig. 3. It can be seen that the damping value of the MRF damper increases by enhancing the applied current.

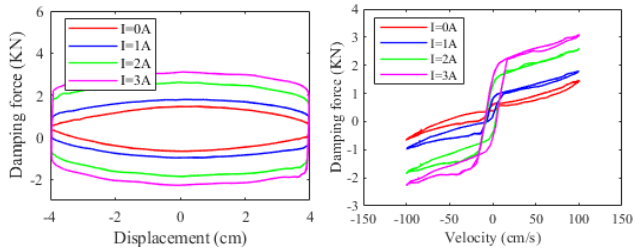

(a) (b)

Fig. 3. (a) The force-displacement and force-velocity hysteresis loops

(b) The force-velocity hysteresis loops

IV. SEMI-ACTIVE CONTROL ALGORITHM FOR FULL VEHICLE SUSPENSION SYSTEM

The proposed control algorithm utilizes the sensor signal of the full-vehicle system and derives the current signal for MR damper. The framework of the proposed controller is shown in Fig. 4.

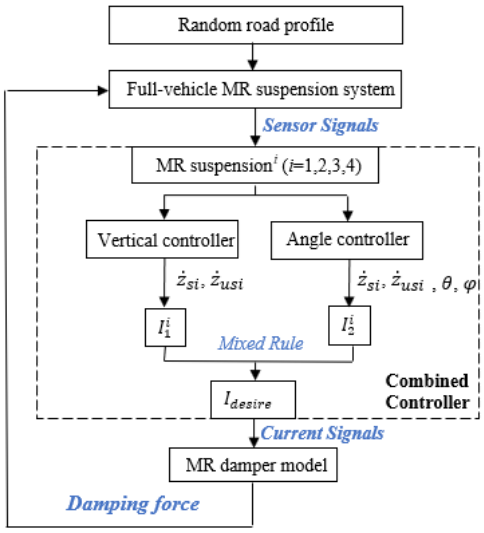

Fig. 4. The framework of full-vehicle system control

In the present work, the proposed control algorithm involves the combination of a vertical controller and an angle controller for each quarter suspension (Fig. 4). The vertical controller applies the sky-hook control method to mitigate the vertical vibration of each suspension and the desired current signals calculated. However, the different vertical motion of each

suspension may induce the position imbalance of the full vehicle body, which generates the pitch and roll motion of vehicle body. The vertical motion, pitch motion and roll motion affect each other, which will cause the vehicle body twist. That is, the different rotation degrees of freedom on the vehicle body cannot be eliminated merely by the vertical control of each single suspension. Consequently, besides the vertical controller for each suspension, a vehicle body angle controller should be further proposed to calculate the attitude compensation induced current for each suspension based on its real-time state (e.g., compression or tension state). The two current signals from sky-hook controller and attitude controller are mixed into a desired current, and it is compared to the limited-boundary to determine the final current signal.

A. Vertical control algorithm for individual suspension

Based on the principle of traditional sky-hook controller, a practical sky-hook control for one signal suspension is modified, by which a current signal is derived by the input sensor signals for sprung mass and unsprung mass.

The sky-hook control algorithm for obtaining the applied current of MR suspension is expressed below,

$$I_{si}=\begin{cases} I_{\max}, \dot{z}_{si}\left(\dot{z}_{si}-\dot{z}_{usi}\right)\geq 0 \\ I_{\min}, \dot{z}_{si}\left(\dot{z}_{si}-\dot{z}_{usi}\right)<0 \end{cases} \tag{12}$$

B. Angle control algorithm for individual suspension

Besides the vertical vibration of the vehicle body, an angle motion based algorithm is proposed for further controlling the full-vehicle attitude. For one quarter suspension, firstly, the real-time state of the suspension should be identified by the roll and pitch angles of the full vehicle system, that is, whether the suspension is under compression or tension state compared to its un-deformed original state; secondly, according to the suspension velocity signal, its following state should be predicted, whether it approaches to its original state (continue compression) or it is away its original state (continue tension); thirdly, a current signal is designed for eliminating the vehicle body angle motion. The process of angle controller is shown in Fig. 5.

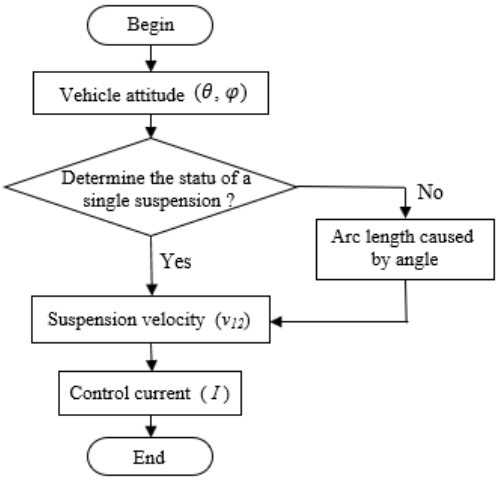

Fig. 5. The process of angle controller

A detailed illustration is explained as follows. Taken the left front wheel as an example, if the body posture leans forward and right, the left front suspension is in compression, compared with its original state. Then by the real-time suspension velocity (v_{12-LF}), its following state can be predicted; if it keeps compression, the maximum current should be applied to attenuate the compression, which is beneficial to compensate the vehicle body's angle motion, and vice versa. It should be noted that, in the case of the pitch and roll angles are in different signs, the angle-induced arc length is calculated and compared to evaluate the suspension state. Consequently, the left front wheel angle control algorithm can be expressed as,

$$\begin{cases} \theta<0,\phi<0\begin{cases} v_{12-LF}<0, I=I_{\max} \\ v_{12-LF}\geq 0, I=0 \end{cases} \\ \theta<0,\phi\geq 0\begin{cases} \left|l_f\cdot\theta\right|\geq\left|\dfrac{b_f}{2}\cdot\phi\right|\begin{cases} v_{12-LF}<0, I=I_{\max} \\ v_{12-LF}\geq 0, I=0 \end{cases} \\ \left|l_f\cdot\theta\right|<\left|\dfrac{b_f}{2}\cdot\phi\right|\begin{cases} v_{12-LF}<0, I=0 \\ v_{12-LF}\geq 0, I=I_{\max} \end{cases} \end{cases} \\ \theta\geq 0,\phi\geq 0\begin{cases} v_{12-LF}<0, I=0 \\ v_{12-LF}\geq 0, I=I_{\max} \end{cases} \\ \theta\geq 0,\phi<0\begin{cases} \left|l_f\cdot\theta\right|\geq\left|\dfrac{b_f}{2}\cdot\phi\right|\begin{cases} v_{12-LF}<0, I=0 \\ v_{12-LF}\geq 0, I=I_{\max} \end{cases} \\ \left|l_f\cdot\theta\right|<\left|\dfrac{b_f}{2}\cdot\phi\right|\begin{cases} v_{12-LF}<0, I=I_{\max} \\ v_{12-LF}\geq 0, I=0 \end{cases} \end{cases} \end{cases} \tag{13}$$

By considering the vertical and angle controllers, the combining rule is defined,

(1) If the current signal of vertical controller and angle controller are respectively I_{max}, then the mixed current is I_{max};

(2) If the current signal of vertical controller and angle controller are respectively I_{min}, then the mixed current is I_{min};

(3) If the current signal of vertical controller and angle controller are respectively I_{max} and I_{min}, then the mixed current is αI_{max}, $\alpha\epsilon(0,1)$.

(4) If the current signal of vertical controller and angle controller are respectively I_{min} and I_{max}, then the mixed current is I_{min}.

By extensive trials, α is adopted as 0.75 for the best performance.

C. State observer for the proposed combine control algorithm

In the proposed controller, vehicle body center accelerations (vertical acceleration, pitch angular acceleration and roll angular acceleration) are real-time monitored. The acceleration signal can be integrated to derive the velocity signal. Considering the frequency of road excitation, low-pass filter is utilized to deal with the acceleration signal and the high-frequency noise signal is deleted. The sprung mass velocity of each individual suspension can be obtained by the geometrical relationship. Similarly, the unsprung mass velocity is also derived. Additionally, the velocity signal of suspension is significant feedback signal. However, in practical, the suspension velocity cannot be directly measured. It can be obtained by the difference between the sprung mass velocity and the unsprung mass velocity.

V. CONTROL PERFORMANCE EVALUATION

A. Sprung mass vibration analysis

To verify the proposed controller effectiveness for the full-vehicle system, the numerical results between passive damper and semi-active MRF damper are compared. The vehicle body center vertical acceleration and angle motion with varying time are shown in Fig. 6-8.

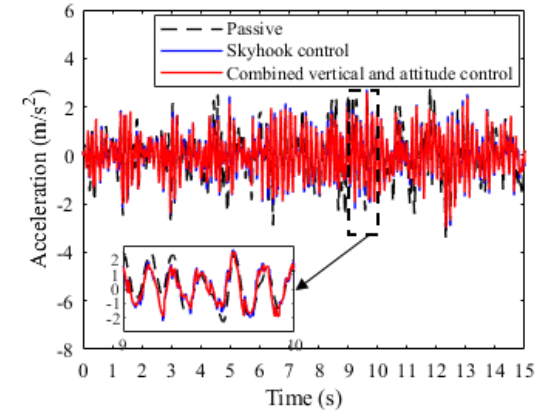

(a)

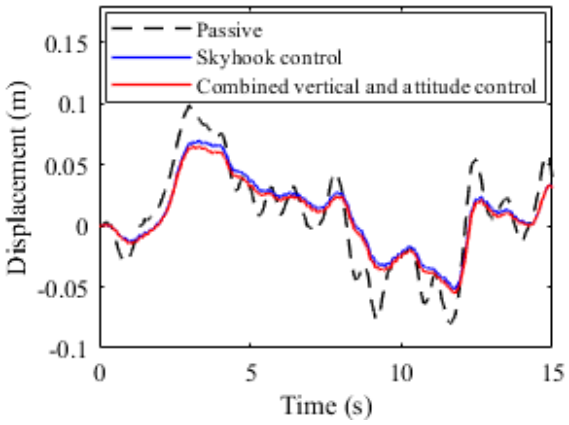

(b)

Fig. 6. Time history of sprung mass center's vertical responses:

(a) acceleration and (b) displacement

The mean square (RMS) values and peak values of the vertical acceleration of the vehicle body with the original passive damper are 1.0059 m/s2 and 3.4447 m/s2, respectively; The RMS value and peak value of pitch angular acceleration are 0.7099 rad/s2 and 2.5398 rad/s2; The RMS value and peak value of roll angle acceleration are 1.6228 rad/s2 and 5.5023 rad/s2 respectively.Compared with the original passive damper, the vertical acceleration RMS values of the semi-active MRF damper using only skyhook and the proposed controller are 0.8062 m/s2 and 0.7825 m/s2, respectively, reducing by 19.85% and 22.21%, with peaks of 3.0844 m/s2 and 3.0162 m/s2, and suppressing by 10.46% and 12.44%; The RMS values of the vehicle acceleration at the pitch angle were 0.4690 rad/s2 and 1.4083 rad/s2, respectively, a decrease of 33.93% and 37.01%, with peaks of 2.0699 rad/s2 and 1.9235 rad/s2, a decrease of 18.49% and 24.27%; The RMS values of the vehicle acceleration for the roll angle were 1.4083 rad/s2 and 1.3694 rad/s2, respectively, a decrease of 13.22% and 15.61%, with peaks of 5.0529 rad/s2 and 4.8861 rad/s2, a decrease of 8.17% and 11.20%.

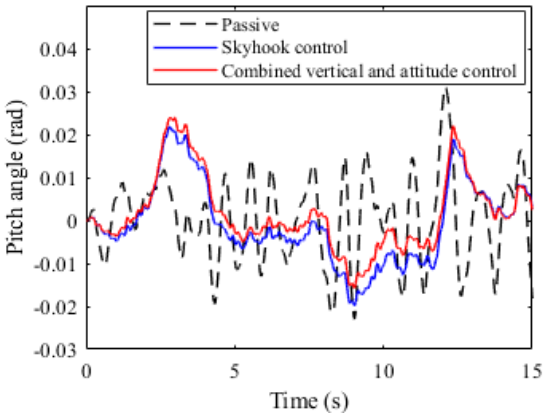

Fig. 7. Time history of the pitch angle of the sprung mass

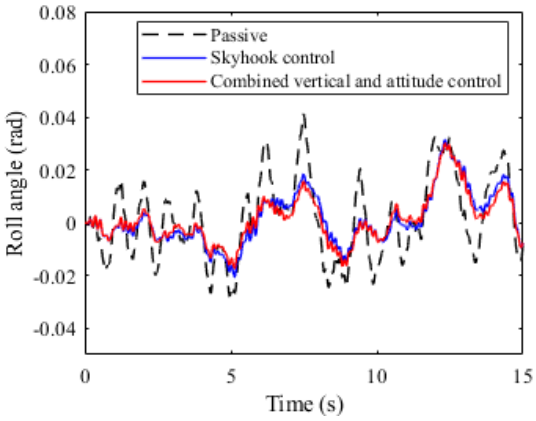

Fig. 8. Time history of the roll angle of the sprung mass

In frequency domain, the power spectrum density (PSD) of vehicle body center acceleration by passive damper and MRF damper is compared in Fig. 9. The sprung mass fundamental frequency is in the range of 1~2Hz. Hence, the PSD curve of vehicle body center focus on the low frequency (e.g., 0-5Hz). As observed in Fig. 9, one dominant peak presents due to the vehicle body resonance, which represents the ride comfort. By the combined controllers of semi-active damper, the peak of body vertical acceleration, pitch angle acceleration and roll angle acceleration are greatly decreased, which represents the ride comfort is enhanced.

B. Suspension and unsprung mass dynamic analysis

Besides the ride comfort evaluation, the holding property should be also concerned. Taking the suspension dynamic travel and tire dynamic loads of the right front wheel as an example. Compared with the passive suspension, the peak value of the dynamic travel by semi-active MRF suspension has been deteriorated, but the maximum value is not more than 7 cm, which is smaller than the dynamic suspension deflection (7-9 cm)for vehicle design requirements [9]. The RMS of tire dynamicload is deteriorated by 21%, which is due to the combined controller replying on the skyhook control of vehicle body vertical acceleration. For enhancing the performance on

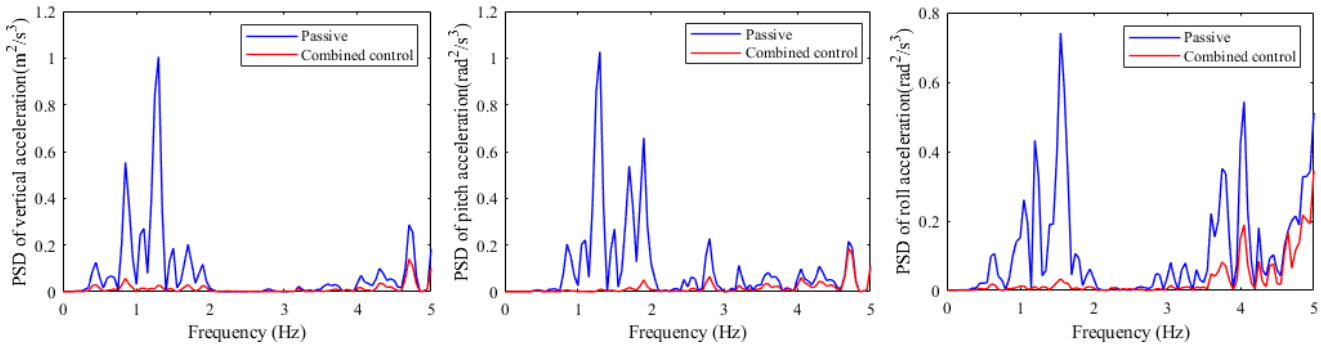

(a) (b) (c)

Fig. 9. Power spectrum density of vehicle body center:(a) vertical acceleration, (b) pitch acceleration and (c) roll acceleration

suspension dynamic travel and tire dynamic load, some other vertical controller may be attempted (e.g., ground hook controller or mixed sky-ground hook controller) in the future.

VI. CONCLUSION

In the present work, a novel control algorithm for full vehicle with magnetorheological suspension is proposed, which aims to simultaneously control the vehicle body's vertical vibration and attitude motion. The proposed controller is a combination of a vertical controller based on skyhook principle and an angle controller by monitoring the dynamic state of MR suspension to compensate the vehicle attitude. Dynamic characteristics of MR damper are experimentally tested, which depicts by a hyperbolic tangent model. Unlike the existing full-vehicle controller in the previous research which merely outputs the control force, the main contribution of the proposed controller is that it can directly derive the current signal, which avoids the operation of complex inverse model of MR damper. The results show that the present controller can both improve the ride comfort and decrease the pitch and roll of the vehicle body. Compared with the original passive damper, the vehicle body center acceleration, pitch angular acceleration and roll angular acceleration under proposed controller are reduced by 22.2%, 37.0% and 15.6%. Furthermore, compared with the merely skyhook vertical control without vehicle body angle compensation, the attitude index is enhanced. This work provides a reference for full-vehicle vertical and rotation motion by MR suspension.

REFERENCES

[1] H. Du, K. Sze, and J. Lam, "Semi-active H-infinity control of vehicle suspension with magneto-rheological dampers," Journal of Sound and Vibration, vol. 283, no. 3-5, pp. 981-996, 2005.

[2] G. Verros, S. Natsiavas, and C. Papadimitriou, "Design optimization of quarter-car models with passive and semi-active suspensions under random road excitation," Journal of Vibration and Control, vol. 11, no. 5, pp. 581-606, 2005.

[3] S.M. Savaresi, and C. Spelta, "Mixed sky-hook and ADD: Approaching the filtering limits of a semi-active suspension," Journal of Dynamic Systems Measurement and Control-Transactions of the ASME, vol. 129, no. 4, pp. 382-392, 2007.

[4] X. Dong, M. Yu, C. Liao, and W. Chen, "Comparative research on semi-active control strategies for magneto-rheological suspension," Nonlinear Dynamics, vol. 59, no. 3, pp. 433-453, 2010.

[5] L. Zong, X. Gong, C. Guo, and S. Xuan, "Inverse neuro-fuzzy MR damper model and its application in vibration control of vehicle suspension system," Vehicle System Dynamics, vol. 50, no. 7, pp. 1025-1041, 2012.

[6] X. Tang, H. Du, S. Sun, D. Ning, Z. Xing, and W. Li, "Takagi-Sugeno Fuzzy Control for Semi-Active Vehicle Suspension With a Magnetorheological Damper and Experimental Validation," IEEE-ASME Transactions on Mechatronics, vol. 22, no. 1, pp. 291-300, 2017.

[7] D. Leng, Z. Zhu, G. Liu, Y. Li. " Neuro fuzzy logic control of magnetorheological elastomer isolation system for vibration mitigation of offshore jacket platforms," Ocean Engineering, vol. 253, no. 111293, 2022

[8] D. Leng, Z. Zhu, K. Xu, Y. Li, G. Liu. "Vibration control of jacket offshore platform through magnetorheological elastomer (MRE) based isolation system," Applied Ocean Research, vol. 114, pp. 102779, 2021.

[9] D. Leng, Y. Yang, K. Xu, Y. Li, G Liu, X. Tian, Y. Xie. "Vibration control of offshore wind turbine under multiple hazards using single variable-stiffness tuned mass damper," Ocean Engineering, vol. 236, pp. 109473, 2021.

[10] J. Yao, S. Taheri, S. Tian, Z. Zhang, and L. Shen, "A novel semi-active suspension design based on decoupling skyhook control," Journal of Vibroengineering, vol. 16, no. 3, pp. 1318-1325, 2014.

[11] R. Wang, F. Sheng, R. Ding, X. Meng, and Z. Sun, "Vehicle attitude compensation control of magneto-rheological semi-active suspension based on state observer," Proceedings of the Institution of Mechanical Engineers Part D-Journal of Automobile Engineering. vol. 235, no. 14, pp. 3299-3313, 2021.

[12] C. Wang, W. Zhao, Z. Luan, Q. Gao, and K. Deng, "Decoupling control of vehicle chassis system based on neural network inverse system," Mechanical Systems and Signal Processing, vol. 106, pp. 176-197, 2018.

[13] S. Lu, Y. Li, S. Choi, L. Zheng, and M. Seong, "Integrated control on MR vehicle suspension system associated with braking and steering control," Vehicle System Dynamics, vol. 49, no. 1-2, pp. 361-380, 2011.

[14] A.H. Ahangarnejad, S. Melzi, and M. Ahmadian, "Integrated vehicle dynamics system through coordinating active aerodynamic control, active rear steering, torque vectoring and hydraulically interconnected suspension," International Journal of Automotive Technology, vol. 20, no. 5, pp. 903-915, 2019.

[15] M. Yu, S. Choi, X. Dong, and C. Liao, "Fuzzy neural network control for vehicle stability utilizing magnetorheological suspension system," Journal of Intelligent Material Systems and Structures, vol. 20, no. 4, pp. 457–466, 2009.

[16] S. Choi, and Y. Han, Magnetorheological Fluid Technology: Applications in Vehicle Systems. Boca Raton, CRC Press, 2012.

[17] D.H. Wang, and W.H. Liao, "Magnetorheological fluid dampers: a review of parametric modelling," Smart Materials and Structures, vol. 20, no. 2, pp. 023001-, 2011.